

Thermal and electrical properties of the Ge:Sb:Te system by photoacoustic and Hall measurements

J. M. Yáñez-Limón, J. González-Hernández,* J. J. Alvarado-Gil, I. Delgadillo,[†] and H. Vargas^{†,‡}

Departamento de Física, Centro de Investigación y de Estudios Avanzados del Instituto Politécnico Nacional, Apartado Postal 14-740 07000, México, Distrito Federal, Mexico

(Received 28 June 1995)

The thermal and electrical properties in the (Ge:Sb:Te) system have been determined using photoacoustic and Hall measurements, respectively. The thermal diffusivity, thermal conductivity, hole concentration, and Hall mobility are analyzed as a function of the tellurium concentration in the bulk alloys. It is found that both the thermal and electrical parameters depend strongly on the alloy composition and on the crystalline structure of the solid compound. The thermal and electrical measured parameters correlate well with the density of holes arising from Ge and/or Sb vacancies.

A description of the equilibrium diagram of bulk Ge:Sb:Te materials was given by Abrikosov and Danilova-Dobriakava¹ more than 20 years ago. These studies reported three ternary stoichiometric compounds with compositions along the GeTe-Sb₂Te₃ pseudobinary line. The atomic composition (Ge:Sb:Te) of those three phases are (15:29:56), (8:34:58), and (22:22:56), all having a stable rhombohedral structure after being prepared from the solidification of the liquids. More recently a fourth stoichiometric ternary compound with elemental composition (40:10:50) also along the pseudobinary line has been reported.² It is found that whereas the (15:29:56) and (8:34:58) ternary (Ge:Sb:Te) alloys present hexagonal structure when prepared from mixtures of the elements in bulk form and then furnaceed in quartz ampules, the (40:10:50) phase has a cubic NaCl structure. The same authors have reported that the (22:22:56) alloy is not a stoichiometric phase. Instead, at this nominal composition, two stoichiometric phases are formed with similar lattice parameters.²

The interest in continuing the investigation of materials in the Ge:Sb:Te system stems from their use in phase-change-erasable optical media, as was first proposed by Ovshinsky in the 1960's.³ Phase-change-erasable optical disks based on this pioneering work are now commercially available from several companies. Phase-change optical disks and drives averaging increasingly wider acceptance primarily because of their capability for direct overwrite and a lower cost structure than competing products. Other chalcogenide materials are being applied in semiconductor memories and threshold switches.³

In order to carry out the three-dimensional calculation of the time-transient behavior under laser irradiation in an optical disk (and thus, to be able to obtain the temper-

ature distributions and the heat-flow balance), thermal constants, such as thermal diffusivity, thermal conductivity, and heat capacity, must be known.^{4,5} To our knowledge, no direct experimental measurements to determine these constants have been carried out in the ternary stoichiometric Ge:Sb:Te phases. In this work we have used photoacoustics and Hall measurements to determine the thermal and electrical properties of the ternary and binary stoichiometric phases in the Ge:Sb:Te system.

Ge:Sb:Te alloys of composition along the GeTe-Sb₂Te₃ pseudobinary line were prepared from mixtures of the elements (99.999% pure) in bulk form with nominal compositions of 1(52:0:48), 2(40:10:50), 3(15:29:56), 4(8:34:58), and 5(0:40:60). The numbers inside the parentheses correspond to the (Ge:Sb:Te) elemental composition and the number in front of the parentheses will be used in the following to identify the sample composition. The mixtures were sealed in evacuated (10–5 Torr) quartz ampules and then heated at 850 °C in a rocking furnace for 3 h. When the furnace was turned off, the ampule was left inside until it reached room temperature. This cooling procedure resulted in a slow solidification of the alloys. A visual insertion of the samples after being removed from the ampule showed that compositions 3, 4, and 5 solidified in ingots composed of single crystals with sizes over 1 cm³, whereas samples 1 and 2 showed much smaller particle sizes with no preferential growth. The structural characteristics were confirmed by x-ray diffraction: Whereas sample 2 shows cubic structure, the rest are in the hexagonal phase² and have hence a well-defined *c* axis. For the photoacoustic, Hall, and x-ray-diffraction measurements, samples were cut and polished into platelets of approximately 1 cm² in area and 0.03 cm in height. Samples

TABLE I. Values of thermal diffusivity α , thermal conductivity k , specific heat dc_p , and carrier thermal conductivity k_e of Ge:Sb:Te alloys. All these values were measured with the heat flux parallel to the *c* axis.

(Ge:Sb:Te)	α (cm ² /s)	k (W/cm K)	dc_p (J/cm ³ K)	k_e (W/cm K)
(52:0:48)	0.0324±0.0002	0.0266±0.0093	0.8209±0.0237	0.0223±0.0002
(40:10:50)	0.0121±0.0006	0.0109±0.0008	0.9037±0.0261	0.0030±0.0003
(15:29:56)	0.0270±0.0014	0.0195±0.0002	0.7044±0.0175	0.0089±0.0002
(8:34:58)	0.0170±0.001	0.0183±0.0017	1.0800±0.0346	0.0147±0.0003
(0:40:60)	0.0160±0.0007	0.0165±0.0011	1.0249±0.0229	0.0103±0.0003

with the c axis perpendicular and parallel to the main surfaces were prepared for the various analyses.

The experimental arrangement used to measure the thermal diffusivity of our samples has been described in previous reports.^{6,7} The open-cell photoacoustic method in the rear-side illumination configuration⁸ was used. The thermal diffusion model of Rosencwaig and Gersho^{9,10} predicts that for an opaque sample of thickness l , the amplitude A of the photoacoustic signal decreases exponentially with the modulation frequency according to

$$A \sim (1/f) \exp(-af^{1/2}), \quad (1)$$

where $a = \pi l^2 / \alpha$. Knowing the coefficient a from the fitting procedure, the thermal diffusivity α is readily obtained.

The specific heat (considered as the product of the density d and the specific heat at constant pressure c_p) was measured using the temperature rise method,¹¹⁻¹³ under continuous white light illumination as follows. After being used for the thermal diffusivity measurements, the samples were black coated on both surfaces using a black ink spray and were suspended by a 1-mm-diam nylon lead in a vacuum sealed Dewar. The Dewar had an optical glass window through which the beam from a 250-W tungsten filament lamp is focused onto the sample surface. The sample temperature rise was recorded by a thermocouple attached to the back surface of the sample using thermal paste. The temperature rise is given by

$$\Delta T = \frac{I_0 \alpha \tau}{lk} (1 - e^{-t/\tau}), \quad (2)$$

where I_0 is the intensity of the incident light beam and $\tau = l dc_p / 2H$ is the rising time. Here, $H = 4\sigma_b T_0^3$, with σ_b the Stefan-Boltzmann constant and T_0 the ambient temperature, is the radiation heat-transfer coefficient. Complementarily, we have also measured the temperature evolution when the illumination is switched off. The product dc_p was obtained by fitting the experimental points to Eq. (2), under maintenance of τ as an adjustable parameter. In order to obtain c_p using the above procedure, the sample density ought to be known. We have measured these densities and we have found that their values are essentially independent of the tellurium concentrations ($d = 5.85 \text{ g/cm}^3$).

To determine the dependence of the thermal conductivity as a function of the tellurium concentration, we have used the definition of the thermal diffusivity, namely, $\alpha = k / dc_p$, and substituted the found values. We were also interested in separating the carrier contribution to the thermal conductivity and we have therefore considered the Wiedemann-Franz law,¹⁴

$$k_e = N_L \sigma T. \quad (3)$$

Here, N_L denotes the Lorenz number, T the temperature, and $\sigma = 1/\rho$ the electrical conductivity. In Table I we summarize the values of the data obtained for α , dc_p , k and k_e .

Finally, we have measured the electrical resistivity of our samples as a function of the tellurium concentration. The measurements were carried out using the four-point

TABLE II. Values of electrical parameters, electrical conductivity σ , hole concentration p , and Hall mobility μ of Ge:Sb:Te alloys.

(Ge:Sb:Te)	σ ($1/\Omega \text{ cm}$) $\times 10^3$	p (cm^{-3}) $\times 10^{20}$	μ ($\text{cm}^2/\text{V s}$)
(52:0:48)	5.00 ± 0.11	7.35 ± 0.31	41.00 ± 1.30
(40:10:50)	0.68 ± 0.07	2.59 ± 0.03	17.17 ± 1.87
(15:29:56)	2.00 ± 0.04	4.10 ± 0.08	29.00 ± 0.91
(8:34:58)	3.30 ± 0.07	3.74 ± 0.07	60.50 ± 1.91
(0:40:60)	2.30 ± 0.08	0.40 ± 0.01	357.00 ± 26.95

van der Pauw method.^{15,16} The Ohmic contacts were achieved by evaporating antimony at the four corners of the square samples. In Table II, the values of σ , p , and μ for all the compositions are summarized.

The thermal diffusivity measured along the c axis, as a function of the tellurium concentration, for the various Ge:Sb:Te alloys is shown in Fig. 1. As can be seen, with the exception of one data point, there is a monotonic decrease in α with the increase in the tellurium concentration. The lower value of α for sample 2 with composition (40:10:50) is related to the different structural phase in which this alloy solidifies when it is prepared. As mentioned above, this material has the face-centered-cubic structure, whereas the other alloys have a hexagonal phase. The thermal diffusivity perpendicular to the c axis was only measured in some of the alloys because of the difficulty of cutting thin samples with that orientation. The measured values in samples with compositions 3, 4, and 5 were 0.0305 ± 0.0004 , 0.0487 ± 0.0005 , and $0.0421 \pm 0.0004 \text{ cm}^2/\text{s}$, respectively. As can be seen, they are larger than the corresponding values of α measured along the c axis. The inset in Fig. 1 shows a typical semi-logarithmic plot of the photoacoustic signal amplitude as

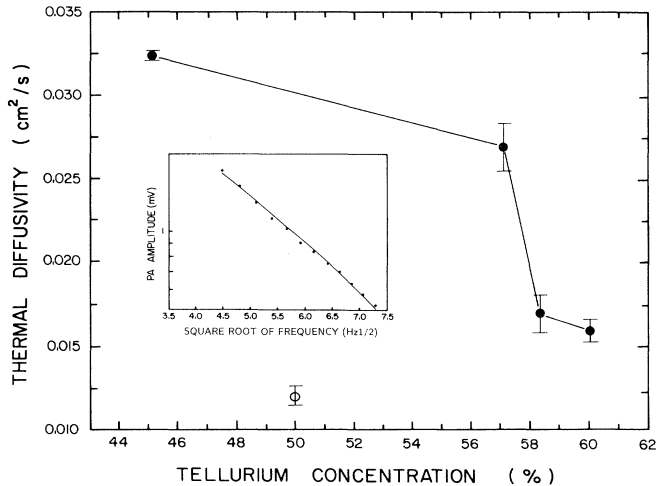


FIG. 1. Thermal diffusivity of the Ge:Sb:Te alloys as a function of the tellurium concentration. The values are measured with the heat flux parallel to the c axis. In the inset, the dependence of the photoacoustic signal amplitude as a function of the frequency square root for the $\text{Ge}_{15}\text{Sb}_{29}\text{Te}_{56}$ alloy is shown. The solid curve represents the fit of the experimental data to Eq. (1) in the text. The value of thermal diffusivity parallel to the c axis is $\alpha = 0.0270 \text{ cm}^2/\text{s}$.

a function of the square root of the modulation frequency of the chopped light for the samples under investigation. The data shown in this inset correspond to a sample with composition (15:29:56) and for a cut with the c axis perpendicular to the main surface, i.e., the heat flow is parallel to the c axis. The solid curve in this inset represents the fitting of the experimental data to Eq. (1). This was the procedure applied to obtain the values of Fig. 1 and Table I.

Figure 2 shows the thermal conductivity, measured along the c axis, of the different alloys as a function of the tellurium concentration. Similar to α , there is a decrease in the thermal conductivity with the increase in the tellurium concentration in the alloys which show the hexagonal phase (see also Table I). Again, the sample with composition (40:10:50) presents a much lower value of k , as indicated by the open circle. Thermal conductivity was only measured along the c axis. In the inset of this figure, we show a typical back surface temperature rise (a) as a function of time, as well as the cooling temperature of the back (b) when illumination is switched off. The data shown in this inset correspond to a 307- μm -thick (15:29:56) sample. The solid line in both curves represents the result of the best fit of the experimental data.

For the samples considered, Fig. 3 shows the hole concentration Hall mobility as a function of the tellurium concentration for samples where the c axis is perpendicular to the surface of the sample. The hole concentration decreases and the Hall mobility increases with the increase in the tellurium concentration. Notice that for the sample in the cubic phase, neither parameter in this figure follows a congruous trend with the rest of the materials having the hexagonal phase.

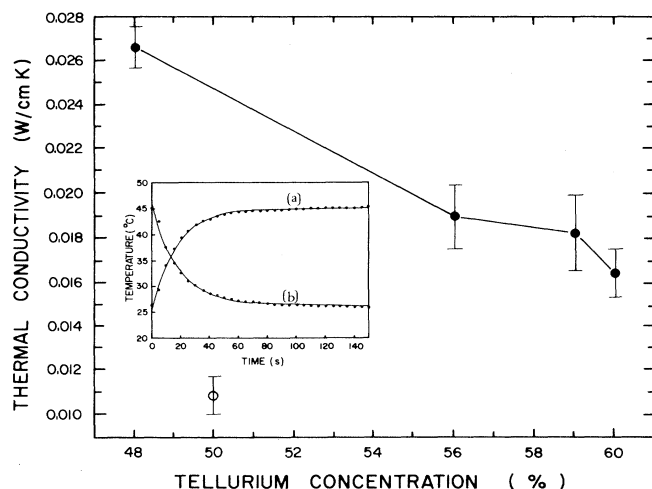


FIG. 2. Thermal conductivity of the Ge:Sb:Te alloys as a function of the tellurium concentration. The measurements are performed with the heat flux parallel to the c axis. The inset shows the back surface temperature evolution of a 307- μm thick black-coated plate of $\text{Ge}_{15}\text{Sb}_{29}\text{Te}_{56}$ sample as a function of time under continuous white light illumination. The solid lines represent the best fits of the data. (a) Rise temperature; (b) evolution of temperature when illumination is switched off. The value of specific heat is $dc_p = 0.7044 \text{ (J/cm}^3 \text{ K)}$.

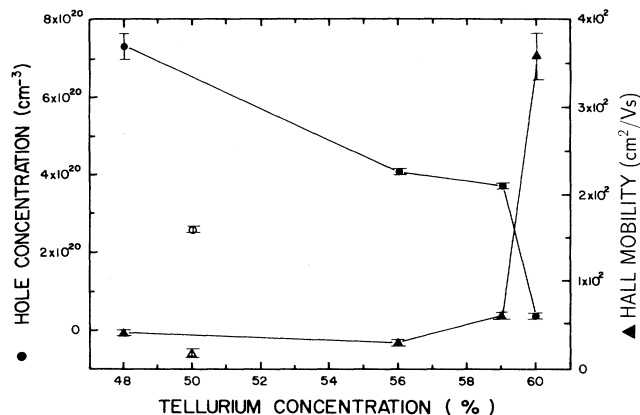


FIG. 3. Hole concentration and Hall mobility, obtained by Hall effect measurements, as a function of the tellurium concentration.

Figure 4 shows the percentage of the thermal conductivity due to the electrical carriers. As is well known, the thermal conductivity of a solid is due to the heat transport by both phonons and carriers.¹⁴ In the case of semiconductors, the carrier concentration is generally small compared with that in a metal or semimetal. In Ge:Sb:Te alloys, the measured carrier concentration is above $1 \times 10^{20} \text{ cm}^{-3}$; therefore, the contribution of the electrical carriers to the thermal conductivity is appreciable. Using the values measured by the Hall effect, the contribution of the free carriers to the thermal conductivity was calculated using the Wiedemann-Franz law.¹⁴ As can be seen in Fig. 4, that percentage has a minimum for the alloy having the cubic phase. This is understood in terms of the lowest hole density for that composition. In conclusion, it is found that both the thermal and electrical parameters depend strongly on the alloy composition and on the crystalline structure of the solid compound. It is observed that in those alloys with the hexagonal phase, the thermal diffusivity and thermal conductivity decrease

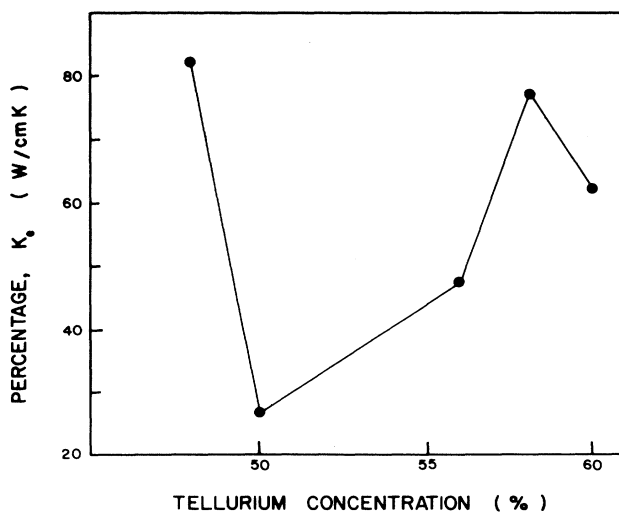


FIG. 4. Percentage of k_c , thermal conductivity due to carriers as a function of the tellurium concentration.

monotonically with the increase in the tellurium concentration. These parameters are much lower for the alloy in the cubic phase.

According to our Hall measurements, all binary and ternary alloys have *p*-type conduction, and the hole concentration decreases with the increase in tellurium concentration. Hall mobility follows an opposite trend. These results can be explained based on the electrically active defects occurring preferentially in the hexagonal structure. Experimental studies in the narrow-band-gap semiconductor GeTe (Ref. 17) show that the structure is not in the range of homogeneity of the alloy, i.e., for a nominal stoichiometric composition, the bulk sample results in the coexistence of free Ge and a GeTe compound in which the Ge exceeds 50%. The stable crystalline phase of this compound is hexagonal and contains a large concentration of holes arising mainly from Ge vacancies. These defects are responsible for the high electrical conductivity. According to previous reports² and in agreement with this work, the amount of vacancies decreases

with increasing substitution of Ge for Sb in the GeTe to form ternary (Ge:Sb:Te) alloys with hexagonal phase. In contrast, the composition (40:10:50) solidifies into a cubic rock-salt structure and has a smaller electrical conductivity. The lower conductivity or smaller free-charge density is probably related to the smaller density of Ge and/or Sb vacancies. The monotonic decrease in the thermal diffusivity and thermal conductivity as a function of tellurium concentration of the sample in the hexagonal phase is understood in terms of the decrease in the density of free charge, which, in turn, is associated with a reduction in the density of the structural defects. The reduction in the defect density not only decreases the number of free charge but also increases its mobility.

The authors are grateful to Ing. Z. Rivera Alvarez for his technical assistance. This work was partially funded by governmental agencies CONACyT (Mexico) and CNPq (Brazil) whose support is greatly acknowledged.

*Present address: Laboratorio de Investigación en Materiales, Centro de Investigación y de Estudios Avanzados-Universidad Autónoma de Querétaro, Centro Universitario, Cerro de las Campanas, 76010 Querétaro, Querétaro, Mexico.

†Present address: Programa Multidisciplinario de Ciencias Aplicadas y Tecnología Avanzada, Centro de Investigación y de Estudios Avanzados del IPN, Apdo. Postal 14-740 07000, México D.F., Mexico.

‡On leave of absence from the University of Campinas, Campinas, S.P., Brazil.

¹N. Kh. Abrikosov and G. T. Danilova-Dobriakava, *Izv. Akad. Nauk SSSR, Neorg. Mater.* **1**, 204 (1965).

²J. González-Hernández, B. S. Chao, D. Strand, S. R. Ovshinsky, D. Pawlik, and P. Gasiorowski, *Appl. Phys. Commun.* **11**, 557 (1992).

³*Disordered Materials Science and Technology, Selected Papers by S. R. Ovshinsky*, edited by D. Adler, B. Schwartz, and M. Silver (Plenum, New York, 1991).

⁴K. A. Rubin, D. P. Birni III, and M. Chen, *J. Appl. Phys.* **71**, 3680 (1992).

⁵T. Ishida, S. Ohara, and N. Akahira, *Jpn. J. Appl. Phys.* **28**,

129 (1989).

⁶H. Vargas and L. C. M. Miranda, *Phys. Rep.* **161**, 45 (1988).

⁷A. M. Mansanares, M. L. Baesso, E. C. da Silva, F. C. G. Gandra, H. Vargas, and L. C. M. Miranda, *Phys. Rev. B* **40**, 7912 (1989).

⁸M. V. Marquezini, N. Cella, A. M. Mansanares, H. Vargas, and L. C. M. Miranda, *Meas. Sci. Technol.* **2**, 396 (1991).

⁹A. Rosencwaig and A. Gersho, *J. Appl. Phys.* **47**, 64 (1975).

¹⁰A. C. Bento, F. C. G. Gandra, E. C. da Silva, and H. Vargas, and L. C. M. Miranda, *Phys. Rev. B* **45**, 5031 (1992).

¹¹S. O. Ferreira, C. Ying An, I. N. Bandeira, L. C. M. Miranda, and H. Vargas, *Phys. Rev. B* **39**, 7967 (1989).

¹²A. M. Mansanares, A. C. Bento, H. Vargas, N. F. Leite, and L. C. M. Miranda, *Phys. Rev. B* **42**, 4477 (1990).

¹³Ichiro Hata, *Rev. Sci. Instrum.* **50**, 292 (1979).

¹⁴C. M. Bhandari and D. M. Rowe, *Thermal Conduction in Semiconductors* (Wiley, New York, 1988), p. 59.

¹⁵L. J. van der Pauw, *Philips Tech. Rev.* **20**, 220 (1958).

¹⁶L. J. van der Pauw, *Philips Res. Rep.* **13**, 1 (1958).

¹⁷L. E. Shelimova, N. Kh. Abrikosov, and V. V. Zhdanova, *Russ. J. Inorg. Chem.* **10**, 650 (1965).